Acta Cryst. (1965). **19**, 401

The Crystal Structure of the Phase β Mg_2Al_3*

BY STEN SAMSON

Gates and Crellin Laboratories of Chemistry,
California Institute of Technology, Pasadena, California, U.S.A.

(*Received* 10 *December* 1964 *and in revised form* 11 *May* 1965)

A determination of the crystal structure of the phase commonly referred to as β Mg_2Al_3 has been carried out and the structure has been refined by three-dimensional, least-squares techniques. The final agreement index R is 0·061 for 1215 reflections. The crystals are cubic, space group $Fd3m$ (O_h^7) with $a_0 = 28{\cdot}239 \pm 0{\cdot}001$ Å. There are approximately 1168 atoms in the unit cell. These are distributed over 23 crystallographically different positions which, as a result of partial disorder, describe 41 different polyhedra. An interesting feature of the disorder is that it results in an increase in the number of icosahedra in the unit of structure, over that found in the idealized ordered model. The unit cube contains 672 icosahedra, 252 Friauf polyhedra, and 244 miscellaneous, more-or-less irregular polyhedra of ligancy 10 to 16.

Introduction

The existence of the β phase in the magnesium–aluminum system was established by Riederer (1936). He proposed on the basis of powder diffraction studies that the structure is hexagonal with $a = 11{\cdot}38$ kX, $c = 17{\cdot}99$ kX, and eight formula units of Mg_5Al_8 per unit cell; the measured density was $\varrho_m = 2{\cdot}23$ g.cm^{-3}. Laves & Möller (1938) concluded, again, from observation of powder patterns, that the β phase is isomorphous with Cu_4Cd_3. Perlitz (1944, 1946) investigated a small fragment of an alloy consisting of 38% Mg and 62% Al by weight, which he found to represent a cubic structure, space group $Fd3m$ (O_h^7), with approximately 1166 atoms per unit cube of edge $a_0 = 28{\cdot}22$ Å. He assumed the composition Mg_2Al_3 and used the density given by Riederer to determine the unit-cell content. Although the exact composition is still not known, the name β Mg_2Al_3 commonly used in the literature will be retained.

A compound with structure apparently similar to that of β Mg_2Al_3 is $NaCd_2$, which is cubic, space group $Fd3m$ (O_h^7), cube edge $a_0 = 30{\cdot}56$ Å (Samson, 1962).

Structure investigations of Cu_4Cd_3, $NaCd_2$, and β Mg_2Al_3 have been under way here for some time. Single crystals of Cu_4Cd_3 were found to be cubic, probable space groups $F\bar{4}3m$ (T_d^2), $F432$ (O^3) or $Fm3m$ (O_h^5), with approximately 1116 atoms per unit cube of edge $a_0 = 25{\cdot}87$ Å; the structure determination is not yet completed. A fairly detailed but not complete picture of the structure of $NaCd_2$ was reported recently (Samson, 1962), and two reasonable trial structures for β Mg_2Al_3 were proposed (Samson, 1964), one of which is identical with that of $NaCd_2$. Up to that date every effort to obtain single crystals of β Mg_2Al_3 had been unsuccessful; the crystals were always twinned. Continued efforts have led to a solution of this problem and to the detailed structure analysis described below.

Experimental

Composition and density

Since no information regarding the exact composition of β Mg_2Al_3 could be found in the literature a partial phase-diagram study was carried out here.

Binary magnesium–aluminum alloys of various compositions were levitated, while molten, in a high-frequency magnetic field inside a vertical glass cylinder, which contained a water-cooled copper mold at the bottom. As soon as the field was shut off the melt dropped into the cooled mold and solidified instantaneously. During this operation the cylinder was kept filled with argon gas that had been dried by passing it slowly through an 8-foot length of pipe (2 inches in diameter) filled with Linde molecular sieve. Each of the very fine-grained and non-segregated alloys thus obtained was annealed at 400 °C in a small alundum crucible inside an evacuated and sealed Pyrex tube. It was then quenched in liquid nitrogen and investigated metallographically as well as with X-ray powder techniques employing crystal-monochromatized copper radiation (Guinier–Hägg camera). The very clear and sharp powder patterns permitted small amounts of adjacent phases to be detected.

The density of each alloy was determined by the method of Archimedes. To reduce possible inclusions of gas bubbles, each specimen was crushed and kept inside a small glass bulb that was suspended with a hair attached to the balance. Three of the alloys, confidently regarded as single-phase samples, were chemically analyzed at a commercial laboratory. The results were as follows:

* Contribution No. 3190 from Gates and Crellin Laboratories. This work was supported in part by a grant GP-1701 from the National Science Foundation and in part with a terminal grant from the Office of Naval Research, Contract No. Nonr-220(33).

Mg 37·83%, Al 62·10%; *i.e.* $Mg_2Al_{2\cdot96}$;
$\varrho_m = 2\cdot249$ g.cm^{-3} (1)

Mg 37·47%, Al 62·49%; *i.e.* $Mg_2Al_{3\cdot01}$;
$\varrho_m = 2\cdot224$ g.cm^{-3} (2)

Mg 36·23%, Al 63·76%; *i.e.* $Mg_2Al_{3\cdot17}$;
$\varrho_m = 2\cdot229$ g.cm^{-3} (3)

These results suggest that the β phase is of slightly variable composition. The phase boundary at the aluminum-rich end has not yet been established, but it seems likely that the β phase can be still richer in aluminum than sample No. 3; Riederer's (1936) composition corresponds to $Mg_2Al_{3\cdot20}$.

The metals used in these preparations as well as in the subsequent experiments were of 99·9% purity.

Single crystals

Initial attempts to obtain single crystals of the β phase were unsuccessful. Crystallites isolated from a variety of slowly solidified melts of about 10 g each and of approximate composition Mg_2Al_3 were always twinned, even after subsequent annealing of the ingots at various temperatures. Although X-ray photographs obtained from such crystallites were useless for the collection of intensity data, they clearly showed the presence of the cubic structure described by Perlitz (1944, 1946).

A large ingot of about 200 g of approximately the same composition as above was prepared. It was melted, solidified, annealed, and crushed several times but again no single crystals could be found. Finally, some small pieces of this alloy were placed in an alundum thimble that terminated at the bottom in a sharp conical tip which rested on a cooling jacket. This assembly was placed inside a resistance furnace that provided a steep temperature gradient, heated above the melting point (>500 °C) of the alloy and then allowed to cool slowly while water was passed through the cooling jacket. The alloy, while heated, was kept in dried argon gas at atmospheric pressure. The pieces of alloy did not melt together, but formed beads of roughly $\frac{1}{2}$ cm or less in diameter. Many of the beads contained needleshaped single crystals of excellent quality for the subsequent X-ray work.

Unit cell and space group

A single crystal was mounted with the needle axis parallel to the axis of rotation. Laue, rotation and heavily exposed Weissenberg photographs of layer lines 0 to 6 showed this axis to be the [011] direction of a face-centered cube having Laue symmetry $m3m$. Only reflections of the type

$$hkl\colon\ h+k,\ k+l,\ (l+h)=2n$$
$$0kl\colon\ (k,\ l=2n),\ k+l=4n$$

were present. Hence, the space group $Fd3m$ was confirmed.

The cell edge was determined from a photograph taken in a precision Weissenberg camera of 10 cm diameter with the film placed in the asymmetric position. Nickel-filtered Cu $K\alpha$ radiation was used and the ambient temperature was 23° ± 1 °C. A Nelson–Riley plot gave $a_0 = 28\cdot239 \pm 0\cdot001$ Å ($\lambda = 1\cdot5418$ Å). The plot was practically horizontal.

The chemical analyses and measured densities of the three samples quoted above give the following unit-cell contents for $a_0 = 28\cdot239$ Å:

$Mg_{475}\ Al_{703}$; 1178 atoms per unit cube (1)

$Mg_{465}\ Al_{699}$; 1164 (2)

$Mg_{451}\ Al_{714}$; 1165 (3)

The lengths of the cube edges were not determined for these samples but a comparison of the clear and extremely sharp powder photographs obtained with the use of the focusing crystal monochromator did not reveal any variation in the line spacings.

Intensity data

Since a thorough inspection of the Weissenberg photographs revealed neither a trace of twinning nor other deficiencies, the crystal seemed well suited for the collection of intensity data with counter techniques. Intensities were measured on a manually operated General Electric XRD 5 diffractometer equipped with a G.E. single-crystal orienter, a copper-target X-ray tube with nickel filter, a xenon-filled proportional counter tube, and SPG-2 counter circuitry. All independent reflections up to $2\theta = 160°$ were measured. The integrated intensity was obtained throughout with the 2θ–θ-scan at a scanning speed of 0·2° per minute. The doublets $\alpha_1\alpha_2$ were always measured together in a single scan. For each reflection the background was determined on either side of the peak from the time required to accumulate 1000 counts with both counter and crystal stationary.

The needle-shaped crystal had a cross-section of $40\mu \times 60\mu$ and was 170μ long; it was always completely bathed in the X-ray beam. The integrated intensities of the 066 and 088 reflections measured at $\chi = 90°$ showed a maximum variation of 10% at various settings of φ. This variation was expected on the basis of calculated absorption effects. In order to minimize absorption errors, the settings of χ and φ were chosen such that all reflections measured were in the same sector of the sphere of reflection and that the variation in φ was at a minimum.

The slow scanning speed was necessary because of the low average intensity of the X-ray reflections. About 100 reflections were measured per day with the diffractometer operated continuously, 24 hours per day, until all 1215 intensity data were obtained.

Refinement of the structure

Two possible structural motifs for β Mg_2Al_3, and the methods used in deriving them, were described in an earlier paper (Samson, 1964). The motif shown in Fig. 6(*b*) of that paper gave rise to persistent, serious dis-

crepancies between observed and calculated structure factors and was rejected; for the other motif, the $NaCd_2$ structure [Fig. 6(*a*)], however, promising agreement was obtained and continued refinement led to the ultimate structure.

The initial trial structure comprised 1192 atoms distributed over the seventeen crystallographically different point sets indicated by asterisks in Table 1. Assignment of magnesium and aluminum atoms to the various sets on the basis of size led to a composition $Mg_{440}Al_{752}$ and a calculated density of 2·28 g.cm^{-3}, in near but not entirely satisfactory agreement with the experimental values. For the initial structure factor calculations differentiation between Mg and Al was not significant since the scattering powers of the two metals are nearly the same. The first stages of refinement were carried out on a Burroughs 220 computer. The structure-factor, least-squares program for cubic space groups, which was written by Dr N. Webb (Webb, 1964), is block-diagonal for the positional parameters but full-matrix for individual isotropic temperature factors and the scale factor. The quantity minimized was $\Sigma\omega(F_o^2-F_c^2)^2$ and the weighting system proposed by Hughes (1941) was used. The scattering factors listed on page 202 of *International Tables for X-ray Crystallography* (1962) were employed. All refinement calculations were carried out with the origin of coordinates placed at the center of symmetry.

After several refinement cycles, apparent convergence was reached; the R value was 0·16 for all observed reflections. This value was far too high to be acceptable in view of the anticipated quality of the data, and two other features were disturbing: the temperature factors for atoms Al(7), Al(14), Mg(19), and Al(21) were considerably higher than those of the other atoms, and the coordinate x of Al(21) had become such that atoms related to one another by a center of symmetry were too close together, about 2·1 Å. The difficulties associated with Al(21) were removed by assigning a population factor of 0·5 to the point set which also reduced the cell content to 1176 atoms, a more reasonable figure.

The remaining three abnormally high temperature factors aroused suspicion of disorder. Nevertheless, several attempts were made to escape the acceptance of a disordered structure with a search for an alternative, reasonable structural motif. If the thirteen positions, or even fewer, that had normal temperature factors, were assumed to be approximately correct, there was very limited reasonable latitude for ordered atomic arrangements to fill the remaining space. Several less attractive but nevertheless reasonable ordered arrangements were tested but each one of them had to be rejected. Confidence was gradually established that the proposed trial structure represented the closest approximation to the real structure of β Mg_2Al_3 that could be arrived at with ordered atomic arrangements.

The deviations from the ordered model were uncovered with the aid of three-dimensional difference maps. Since all atoms except Al(1) and Al(2) are repres-

Table 1. *The final parameters of* β Mg_2Al_3

The origin of coordinates is at $\frac{1}{8}\frac{1}{8}\frac{1}{8}$ from the center ($\bar{3}m$); see *International Tables for X-ray Crystallography* (1952) page 340. Blank spaces in columns (*a*) and (*b*) indicate 100 % occupancy. The occupancies shown in column (*a*) and the temperature factors in column B_a correspond to the synthesized model $Mg_{448}Al_{720}$; in columns (*b*) and B_b are listed the values obtained by including the occupancies as refinable parameters.

Atom				Occupancy, %		Temperature factor (Å²)				
No.	Kind	Point	set	(*a*)	(*b*)	B_a	B_b	x	y	z
1*	Al	192(*i*)	*xyz, etc.*			1·12(4)	1·10(4)	0·1468(1)	0·2149(1)	0·4214(1)
2*	Al	96(*h*)	$\frac{1}{8}$, x, $\frac{1}{4}-x$, *etc.*			1·20(4)	1·19(4)	−0·0117(1)		
3*	Al	96(*g*)	*xxz, etc*			1·05(5)	1·02(5)	0·1465(1)		0·2179(1)
4*	Mg	96(*g*)	*xxz, etc.*			1·22(5)	1·22(5)	0·0681(1)		0·2025(1)
5*	Al	96(*g*)	*xxz, etc.*			1·60(5)	1·57(5)	0·2174(1)		0·4886(1)
6*	Mg	96(*g*)	*xxz, etc.*			1·66(6)	1·63(6)	0·0440(1)		0·3144(1)
7*	Al	96(*g*)	*xxz, etc.*	50·0	53·6 ± 1·9	1·86(10)	2·20(18)	0·2175(2)		0·6472(2)
8	Al	96(*g*)	*xxz, etc.*	25·0	22·6 ± 1·2	2·80(26)	2·36(36)	0·1742(4)		0·7520(5)
9	Al	96(*g*)	*xxz, etc.*	16·7	12·1 ± 0·9	1·72(26)	0·41(37)	0·2351(5)		0·8543(7)
10	Al	96(*g*)	*xxz, etc.*	8·3	9·8 ± 1·9	1·75(61)	2·8(1·4)	0·2081(10)		0·6678(15)
11*	Mg	96(*g*)	*xxz, etc.*	75·0	83·6 ± 3·1	1·80(10)	1·94(11)	0·1318(1)		0·4929(2)
12	Al	96(*g*)	*xxz, etc.*	25·0	15·5 ± 2·9	1·50(21)	0·30(51)	0·1416(4)		0·4864(5)
13	Mg	96(*g*)	*xxz, etc.*	50·0	47·5 ± 2·2	2·74(14)	2·44(23)	0·1792(2)		0·5889(3)
14*	Al	96(*g*)	*xxz, etc.*	50·0	51·6 ± 1·9	1·10(8)	1·20(16)	0·1809(1)		0·5661(2)
15*	Mg	48(*f*)	*x*00, *etc.*			1·50(8)	1·46(8)	0·1354(2)		
16*	Al	32(*e*)	*xxx, etc.*			0·97(7)	0·94(7)	0·2152(1)		
17*	Mg	32(*e*)	*xxx, etc.*			1·25(8)	1·24(8)	0·3162(1)		
18*	Mg	32(*e*)	*xxx, etc.*			1·54(9)	1·51(8)	0·3808(1)		
19*	Mg	32(*e*)	*xxz, etc.*†	50·0	44·3 ± 13·6	0·11(30)	0·02(85)	0·4327(3)		0·4474(4)
20	Al	32(*e*)	*xxz, etc.*†	25·0	45·1 ± 13·8	0·40(34)	2·66(92)	0·4472(7)		0·4207(12)
21*	Al	32(*e*)	*xxx, etc.*	50·0	51·4 ± 1·6	0·75(13)	1·32(18)	0·6044(2)		
22*	Al	16(*c*)	$\frac{1}{8}\frac{1}{8}\frac{1}{8}$, *etc.*			1·19(9)	1·18(9)			
23*	Mg	8(*b*)	$\frac{1}{2}\frac{1}{2}\frac{1}{2}$, *etc.*			1·55(17)	1·24(16)			

* Positions are identical with those assumed for the initial trial structure.

† Notation 32(*e*) is used rather than 96(*g*) to indicate that these atoms are displaced from the diagonal *xxx* where they were initially assumed.

ented in the plane $X=Y$, the difference summation was evaluated only in this section. The first map pointed to a number of modifications to the structure: (1) the population parameter of Al(7) should be reduced to about 0·5; (2) two additional point sets of the kind 96(*g*), each with occupancy considerably less than 0·5, should be incorporated [Al(8) and Al(9), Table 1]; (3) atoms Al(14) and Mg(19) should each be apportioned to two point sets of the kind 96(*g*); the added sets were those of Mg(13) and Al(20). The occupancy of 0·5 for Al(21) seemed to be correct.

Subsequent least-squares refinements of this revised model led to an R value of 0·09. During these refinements, additional adjustments of the population factors for the disordered atomic arrangement were made as suggested by the shifts in the temperature parameters. A second difference map indicated that Al(10) should be added with a low population factor and that the atoms Mg(11) should be apportioned to two 96-fold point sets; accordingly Al(12) was added to the atom list (Table 1) which is now complete. Identification of the kind of atoms in the disordered positions was not made until later and at this stage was not essential.

Since discrimination between population factors and temperature factors, with the use of least-squares techniques as applied above, was bound to be more-or-less qualitative and each structure-factor, least-squares cycle required approximately eight hours of computer time on the Burroughs 220, further refinement was postponed. The approximate structural parameters were at this stage used as a basis for the synthesis of the disordered model described in detail in a later section. The most important arguments leading to that model are as follows:

If the set of points assigned to Al(21) is only 50% occupied there is just sufficient space to accommodate Mg(13) and Al(14) in such a way that the coordination shell around each Al(21), which was initially irregular, becomes a slightly distorted icosahedron. With this most reasonable atomic configuration, the occupancies of Mg(13), Al(14), Al(7), and Mg(19) must be 50% (or less) to avoid unreasonably short bond distances. Al(7) and Mg(19) then constitute four Friauf polyhedra that occupy only half the number of centers described by the point set 8*b*, $\frac{111}{222}$, *etc.*; around the other half the coordination shells must be made up by Al(8), Al(9), Al(10), and Al(20). Neither Al(9) nor Al(10) can furnish a complete coordination shell of ligancy twelve, as required by the space-group symmetry, without causing unreasonably short distances between atoms of the same set; both kinds of atom are located in 'forbidden' areas of the packing map (Samson, 1964). Of Al(9) no more than six atoms may occur around a center, while of Al(10) a maximum of only four is possible. A reasonable packing that accounts for the approximately correct number of atoms per unit cube cannot be achieved by placing a coordination shell of ligancy four, six, or ten around any one center ($\frac{111}{222}$, *etc.*). It seems therefore necessary for at least three kinds of atom to be employed simultaneously for each of the four coordination shells. The shell that yields the maximum number of atoms was found to be the pentagonal prism with two atoms at the poles and two atoms out from the centers of two of the prism faces (see description of the disordered model). Four such prisms accommodated in the unit of structure, each consisting of 6 Al(8), 4 Al(9), 2 Al(10), and 2 Al(20), require that the population factors of Mg(11) and Al(12) be 0·75 and 0·25, respectively. The eleven occupancies thus obtained are listed in column (*a*) of Table 1. It will be shown later (see especially the last section) that these occupancies are structurally very reasonable.

Assignment of magnesium and aluminum to the various point sets was made on the basis of atomic radii. The model accounts for 1168 atoms per unit cube and $\varrho_{calc}=2{\cdot}235$ g.cm^{-3}, in excellent agreement with the experimental results. The composition corresponds to Mg_{448} Al_{720} or Mg_2 $Al_{3\cdot22}$.

The least-squares refinement was then continued with the Institute's IBM 7040–7094 computing system (Webb, Duchamp & Marsh, unpublished; see also Webb, 1964), which in the meantime had become operational. The quantity minimized was again $\Sigma\omega(F_o^2-F_c^2)^2$; full shifts were used and weights and scattering factors were the same as those employed before. The eleven partial occupancies given in column (*a*) of Table 1 were introduced during the first six cycles, but they were not included in the full matrix as refinable parameters. Convergence was rapid and resulted in an R index of 0·061. The positional parameters, changed to place the origin of coordinates at $\frac{1}{8}$, $\frac{1}{8}$, $\frac{1}{8}$ from the center of symmetry*, are listed in Table 1 and the temperature factors are given in column B_a of that Table.

Three more refinement cycles with the eleven occupancies included as refinable parameters in the now 72×72 full matrix resulted in the occupancies given in column (*b*) and the temperature factors shown in column B_b of Table 1; the positional parameters came out to be practically unchanged and R was now 0·059; that is, insignificantly smaller.

Columns (*a*), (*b*), and B_a and B_b in Table 1 confirm the anticipated interactions between some of the population factors and the temperature factors. The occupancies for Al(9) and Al(12) have decreased, but this reduction in scattering matter has been compensated by a drastic decrease of the temperature factors. A similar effect, but in reverse direction, is observed for Al(20); here, the occupancy has nearly doubled. No structurally reasonable way was found to accommodate more than eight atoms of Al(20).

The slightly-higher-than-normal temperature factors for Al(8) and Mg(13) are very likely due to small dis-

* While for this space group (*Fd*3*m*) all calculations involving structure factors are most conveniently done with the origin of coordinates placed at the center of symmetry, the alternative origin, at $\frac{1}{8}$, $\frac{1}{8}$, $\frac{1}{8}$ from this center, is most convenient for the description of the atomic arrangement.

placements not accounted for in the model. Displacement of Mg(13) is reflected in the rather short distance, 2·509 Å, for Mg(13)–Al(10) in Table 3. The packing map (see later) suggests that the appropriate positional parameters for this atom are 8% of the time in between those given for Mg(13) and Al(14), but no attempt was made to resolve this problem with further refinements. The synthesized model with occupancies according to column (*a*) of Table 1 seems to represent the closest approach to the real structure that can be obtained with the data used; the exact distribution of the magnesium and aluminum atoms cannot, of course, be determined with certainty.

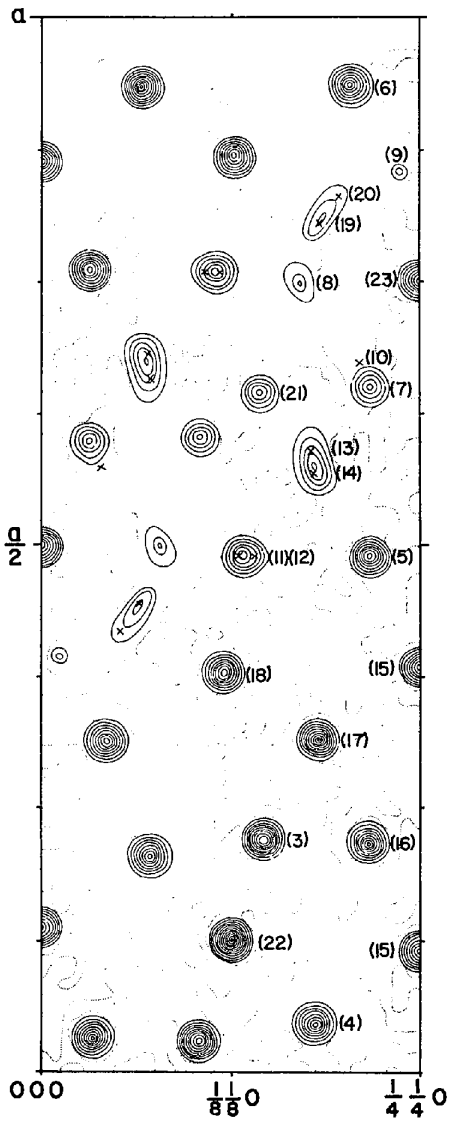

Fig. 1. A Fourier section representing the (110) plane passing through the origin of the cube. The number in parentheses to the right of each peak is the atom number. The pairs of atoms Mg(11)–Al(12), Mg(13)–Al(14), and Mg(19)–Al(20) as well as Al(10) are marked out with crosses. The center of the peak (22) represents the center of symmetry at $\frac{1}{8}\frac{1}{8}\frac{1}{8}$.

The calculated structure factors (origin of coordinates at the center of symmetry) given in Table 2 are those from the final least-squares cycle for the synthesized model (occupancies according to column *a*). The interatomic distances are listed in Table 3. A Fourier section representing the (110) plane passing through the origin of the cube (at $\frac{1}{8}, \frac{1}{8}, \frac{1}{8}$ from the center of symmetry) is shown in Fig. 1.

Description of the structure

The idealized ordered model

The predominating coordination polyhedron about the magnesium atoms consists of two integral parts: a truncated tetrahedron bounded by four triangles and four hexagons [Fig. 2(*a*), (*b*)] and a regular tetrahedron of atoms placed out from the centers of the four hexagons [Fig. 2(*c*)]. This composite coordination shell of 16 atoms is the Friauf polyhedron (see also Samson, 1958, 1961, 1962). Five Friauf polyhedra of three crystallographic kinds (*F*1, *F*2 and *F*3) share hexagons [Fig. 3(*a*)] to form a complex of 47 atoms, the *VF* polyhedron shown in Figs. 3(*b*) and 3(*c*). This polyhedron has crystallographic *mm* symmetry; one of the two mirror planes is seen to be perpendicular to the approximate fivefold axis.

A packing map representing such a mirror plane, the (110) plane passing through the origin of the cube, is shown in Fig. 10, in which the origin of coordinates (lower left star) is placed at $\frac{1}{8}, \frac{1}{8}, \frac{1}{8}$ from the center of symmetry.

Six *VF* polyhedra are arranged about the vertices of an octahedron, producing four additional Friauf polyhedra, *F*4, located at the vertices of a regular tetrahedron and sharing hexagons with polyhedra *F*1. The resulting 234-atom complex, comprising 34 Friauf polyhedra and having symmetry T_d, is shown in Fig.4; the twelve outer Friauf polyhedra are of the type *F*3 and the dark ones are of the type *F*4 (see also Fig. 10).

A second such T_d complex can now be meshed with the first one as shown in Fig. 5; these two complexes share hexagonal faces of the *F*2 polyhedra and are related to one another by a diamond glide. Three more T_d complexes can be added in a similar fashion. Each T_d complex is accordingly connected with four others that are arranged about the vertices of a regular tetrahedron (Fig. 7). As can be seen in Figs. 6 and 7, three Friauf polyhedra *F*3, each of which belongs to a different T_d complex, have one edge in common on the threefold axis passing through the dark hexagon of an *F*4 polyhedron. The two vertices on this edge are occupied by the atoms Mg(18) and Mg(19), as can be seen in Figs. 10 and 11.

Continued stacking of T_d complexes leads to an infinite three-dimensional network in which each T_d complex of 234 atoms shares atoms with four others so as to reduce the average number of atoms per T_d complex to 144. The cubic unit of structure contains eight T_d complexes arranged about points of the set

Table 2. *Observed and calculated structure factors*

Each group of three columns contains, from left to right, indices *l*, observed structure factors, and calculated structure factors. The unobserved values are marked with < signs. The origin of coordinates is at the center of symmetry.

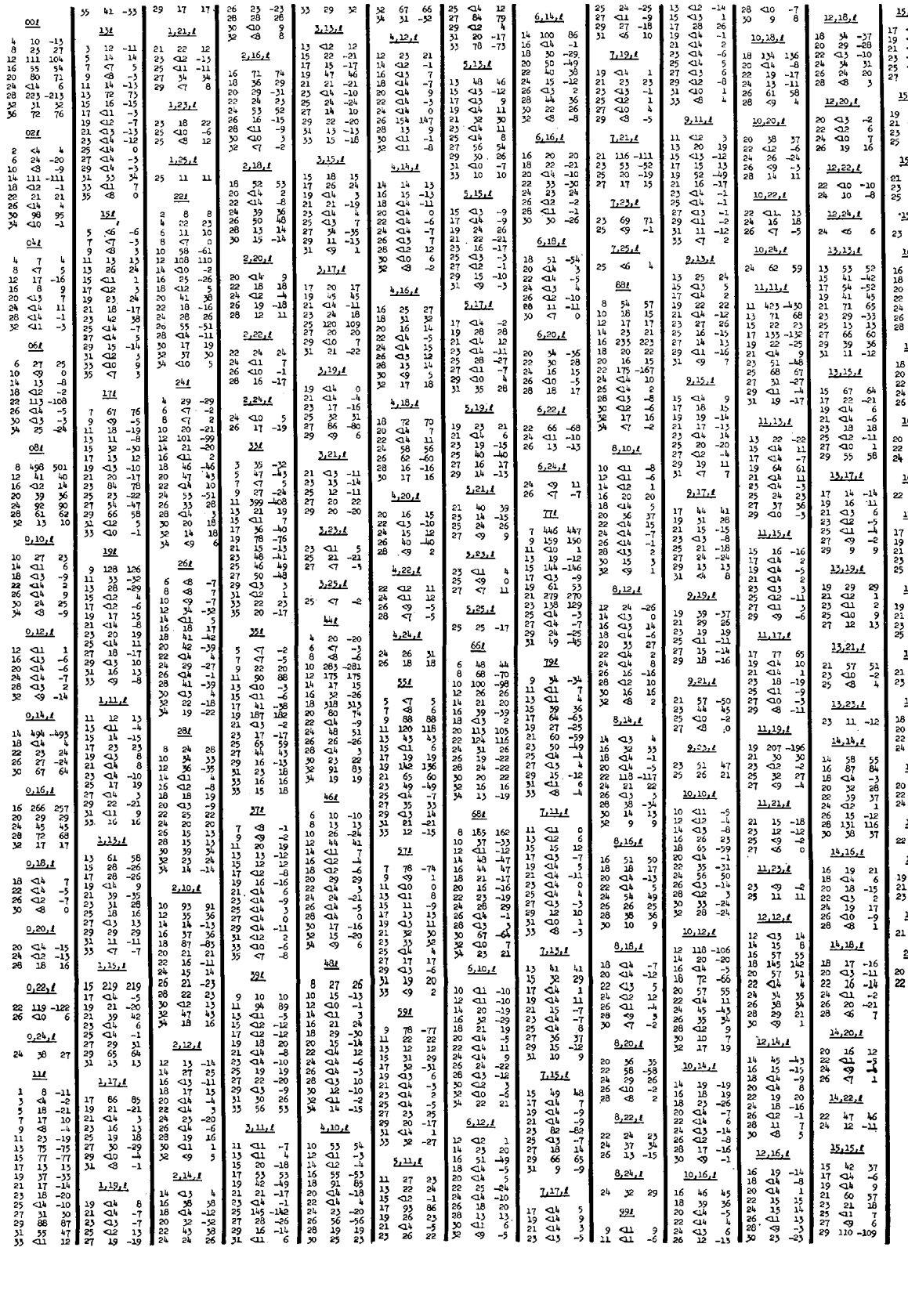

Table 3. *Interatomic distances and bond numbers*

The calculated valences are listed in Tables 4, 5, 8 and 9. The standard deviation in the distances involving Al(10) is ~0·05 Å; all other standard deviations vary between 0·005 and 0·025 Å.

Kind of Atom	Ligancy	Distance Å	Bond No. n
Al(1)	1 Al (1)	2.725	0.415
	1 Al (1)	2.719	0.425
	1 Al (2)	2.705	0.448
	1 Al (3)	2.696	0.464
	1 Mg(4)	3.235	0.092
	1 Mg(4)	3.200	0.105
	1 Al (5)	2.754	0.372
	1 Mg(6)	3.174	0.116
	1 Mg(15)	3.240	0.090
	1 Mg(17)	3.268	0.081
	1 Mg(18)	3.038	0.195
and			
(a)	1 Mg(11)	3.127	0.139
	12, icosahedron (1a)		
or			
(b)	1 Al (12)	2.773	0.345
	12, icosahedron (1b)		
Al(2)	2 Al (1)	2.705	0.448
	2 Mg(4)	3.232	0.093
	2 Al (5)	2.755	0.370
	2 Mg(6)	3.150	0.127
	1 Mg(11)	3.061	0.178
	1 Mg(13)	3.143	0.130
	1 Al (14)	2.735	0.400
and			
(a)	1 Mg(11)	3.061	0.178
	12, icosahedron (2a)		
or			
(b)	1 Al (12)	2.862	0.246
	12, icosahedron (2b)		
Al(3)	2 Al (1)	2.696	0.464
	2 Al (3)	2.853	0.254
	1 Mg(4)	3.161	0.122
	2 Mg(4)	3.139	0.132
	2 Mg(15)	3.190	0.109
	1 Al (16)	2.746	0.383
	1 Mg(17)	3.150	0.127
	1 Al (22)	2.761	0.362
	12, icosahedron (3)		
Mg(4)	2 Al (1)	3.235	0.092
	2 Al (1)	3.200	0.105
	2 Al (2)	3.232	0.093
	1 Al (3)	3.161	0.122
	2 Al (3)	3.139	0.132
	2 Al (5)	3.181	0.113
	1 Al (22)	3.156	0.124
	2 Mg(4)	3.318	0.104
	1 Mg(6)	3.303	0.110
	1 Mg(15)	3.314	0.106
	16, Friauf polyhedron F2		
Al(5)	2 Al (1)	2.754	0.372
	2 Al (2)	2.755	0.370
	2 Mg(4)	3.181	0.113
	1 Al (5)	2.601	0.668
	2 Mg(6)	3.060	0.179
	1 Mg(15)	3.192	0.108
and			
(a)	1 Mg(11)	3.424	0.044
	1 Mg(13)	3.215	0.099
	12, icosahedron (5a)		
or			
(b)	1 Mg(11)	3.424	0.044
	1 Al (14)	2.628	0.603
	12, icosahedron (5b)		
or			
(c)	1 Al (12)	3.031	0.128
	1 Al (14)	2.628	0.603
	12, icosahedron (5c)		
Mg(6)	2 Al (1)	3.174	0.116
	2 Al (2)	3.150	0.127
	2 Al (5)	3.060	0.179
	2 Al (7)	3.200	0.105
	2 Al (14)	3.271	0.080
	1 Mg(18)	3.540	0.044
	1/3 Mg(19)	3.868	1/3 · 0.013
	2/3 Mg(19)	3.413	2/3 · 0.072
	1 Mg(4)	3.303	0.110
	1 Mg(6)	3.516	0.049
	2 Mg(11)	3.088	0.251
	16, Friauf polyhedron F3		
Mg(6)	2 Al (1)	3.174	0.116
	2 Al (2)	3.150	0.127
	1 Mg(4)	3.303	0.110
	2 Al (5)	3.061	0.179
	1 Mg(6)	3.516	0.049
	2 Mg(13)	3.399	0.076
	1 Mg(18)	3.540	0.044
and			
(a)	2 Mg(11)	3.088	0.251
	1 Al (20)	3.021	0.208
	14, polyhedron F3a		
or			
(b)	2 Al (8)	3.440	0.042
	2 Al (12)	3.142	0.131
	15, polyhedron F3b		
or			
(c)	1 Al (9)	2.573	1.162
	2 Mg(11)	3.088	0.251
	14, polyhedron F3c		
or			
(d)	2 Al (8)	3.440	0.042
	1 Al (9)	3.289	0.074
	2 Al (12)	3.142	0.131
	16, polyhedron F3d		
Al(7)	2 Mg(6)	3.200	0.105
	1 Al (7)	2.598	0.676
	2 Al (7)	2.807	0.302
	2 Mg(11)	3.126	0.139
	1 Al (14)	2.715	0.432
	2/3 Mg(19)	3.305	2/3 · 0.070
	2/3 Mg(19)	3.046	2/3 · 0.189
	2/3 Mg(19)	2.785	2/3 · 0.515
	1 Al (21)	2.872	0.236
	1 Mg(23)	3.181	0.112
	12, icosahedron (7)		
Al(8)	2 Mg(6)	3.440	0.042
	2 Al (8)	2.948	0.177
	1 Al (9)	2.728	0.411
	1 Al (12)	2.648	0.558
	2 Mg(13)	3.170	0.118
	1 Mg(18)	3.738	0.013
	1 Mg(23)	3.026	0.204
and			
(a)	1 Al (9)	2.728	0.411
	1 Al (10)	2.736	0.398
	12, icosahedron (8a)		
or			
(b)	1 Al (8)	3.104	0.097
	11, polyhedron (8b)		
Al(9)	1 Mg(6)	3.289	0.074
	1 Mg(6)	2.573	1.162
	2 Al (8)	2.728	0.411
	1 Al (9)	3.568	0.016
	1 Al (10)	3.048	0.120
	2 Mg(11)	3.396	0.049
	2 Mg(13)	3.304	0.070
	1 Al (20)	2.562	0.776
	1 Mg(23)	3.005	0.221
	12, polyhedron (9)		
Al(10)	1 Al (8)	2.736	0.398
	2 Al (9)	3.048	0.120
	1 Al (10)	3.345	0.039
	2 Mg(11)	3.211	0.100
	1 Mg(13)*	(2.509)	(0.951)
	2 Mg(13)	3.480	0.036
	2 Al (20)	2.694	0.468
	1 Mg(23)	2.862	0.383
	12, polyhedron (10)		

*See text regarding possible displacement of Mg(13).

Kind of Atom	Ligancy	Distance Å	Bond No. n
Mg(11)	2 Al (1)	3.127	0.139
	2 Al (2)	3.061	0.179
	1 Al (5)	3.424	0.044
	2 Mg(6)	3.088	0.251
	1 Mg(18)	3.203	0.160
and			
(a)	2 Al (9)	3.396	0.049
	2 Mg(13)	2.914	0.490
	1 Al (14)	2.851	0.400
	13, polyhedron (11a)		
or			
(b)	1 Al (9)	3.396	0.049
	1 Al (10)	3.211	0.100
	2 Mg(13)	2.914	0.490
	1 Al (14)	2.851	0.400
	1 Al (20)	2.971	0.252
	14, polyhedron (11b)		
or			
(c)	2 Al (7)	3.126	0.139
	1 Mg(13)	3.307	0.109
	2 Al (14)	3.151	0.126
	1/3 Mg(19)	2.878	1/3 · 0.562
	2/3 Mg(19)	3.346	2/3 · 0.093
	1 Al (21)	3.333	0.040
	15, polyhedron (11c)		
Al(12)	2 Al (1)	2.773	0.345
	2 Al (2)	2.862	0.246
	1 Al (5)	3.031	0.128
	2 Mg(6)	3.142	0.131
	1 Al (8)	2.648	0.558
	2 Mg(13)	3.158	0.123
	1 Al (14)	2.745	0.385
	1 Mg(18)	3.114	0.146
	12, icosahedron (12)		
Mg(13)	2 Al (2)	3.143	0.130
	1 Al (5)	3.215	0.099
	2 Mg(6)	3.399	0.076
	1 Mg(11)	3.307	0.109
	2 Mg(13)	3.610	0.034
	2 Al (14)	3.164	0.120
	1 Al (21)	3.020	0.134
and			
(a)	2 Al (8)	3.170	0.118
	2 Al (12)	3.158	0.123
	15, polyhedron (13a)		
or			
(b)	1 Al (10)*	(2.509)	(1.485)
	2 Mg(11)	2.914	0.490
	14, polyhedron (13b)		
or			
(c)	1 Al (8)	3.170	0.118
	1 Al (9)	3.304	0.070
	1 Mg(11)	2.914	0.490
	1 Al (12)	3.158	0.123
	15, polyhedron (13c)		
or			
(d)	1 Al (8)	3.170	0.118
	1 Al (9)	3.304	0.070
	1 Al (10)	3.480	0.036
	1 Mg(11)	2.914	0.490
	1 Al (12)	3.158	0.123
	16, Friauf polyhedron F7		
Al(14)	2 Al (2)	2.735	0.400
	1 Al (5)	2.628	0.603
	2 Mg(6)	3.271	0.080
	1 Al (7)	2.715	0.432
	2 Mg(11)	3.151	0.126
	2 Mg(13)	3.164	0.120
	1 Al (21)	2.652	0.550
and			
(a)	1 Mg(11)	2.851	0.400
	12, icosahedron (14a)		
or			
(b)	1 Al (12)	2.745	0.385
	12, icosahedron (14b)		

*See note under Al (10) above.

Table 3 (*cont.*)

Kind of Atom	Ligancy	Distance Å	Bond No. n
Mg(15)	4 Al (1)	3.240	0.090
	4 Al (3)	3.190	0.109
	2 Al (5)	3.192	0.108
	2 Al (16)	3.163	0.120
	2 Mg(4)	3.314	0.106
	2 Mg(17)	3.288	0.117
	16, Friauf polyhedron F1		
Al(16)	3 Al (3)	2.746	0.383
	3 Mg(15)	3.163	0.120
	3 Al (16)	2.778	0.339
	3 Mg(17)	3.116	0.145
	12, icosahedron (16)		
Mg(17)	6 Al (1)	3.268	0.081
	3 Al (3)	3.150	0.127
	3 Al (16)	3.116	0.145
	3 Mg(15)	3.288	0.117
	1 Mg(18)	3.158	0.192
	16, Friauf polyhedron F4		
Mg(18)	6 Al (1)	3.038	0.195
	3 Mg(6)	3.540	0.044
	1 Mg(17)	3.158	0.192
and (a)	1 Mg(19)	2.799	0.762
	3 Mg(11)	3.206	0.160
	14, polyhedron (18a)		
or (b)	3 Mg(11)	3.206	0.160
	1 Al (20)	2.880	0.358
	14, polyhedron (18b)		
or (c)	3 Al (8)	3.738	0.013
	3 Al (12)	3.114	0.146
	16, Friauf polyhedron F6		
Mg(19)	1 Mg(6)	3.868	0.013
	2 Mg(6)	3.413	0.072
	2 Al (7)	2.785	0.515
	2 Al (7)	3.305	0.070
	2 Al (7)	3.046	0.189
	1 Mg(11)	2.878	0.562
	2 Mg(11)	3.346	0.093
	1 Mg(18)	2.799	0.762
	1 Mg(23)	3.072	0.267
	14, polyhedron (19)		
Al(20)	1 Mg(6)	3.021	0.208
	2 Al (9)	2.562	0.776
	2 Al (10)	2.694	0.468
	1 Mg(11)	3.754	0.013
	2 Mg(11)	2.971	0.252
	1 Mg(18)	2.880	0.358
	1 Mg(23)	3.078	0.167
	10, polyhedron (20)		
Al(21)	3 Al (7)	2.872	0.236
	3 Mg(11)	3.333	0.040
	3 Mg(13)	3.020	0.134
	3 Al (14)	2.652	0.550
	12, icosahedron (21)		
Al(22)	6 Al (3)	2.761	0.362
	6 Mg(4)	3.156	0.124
	12, icosahedron (22)		
Mg(23)	12 Al (7)	3.181	0.112
	4 Mg(19)	3.072	0.267
	16, Friauf polyhedron F5		
Mg(23)	6 Al (8)	3.026	0.204
	4 Al (9)	3.005	0.221
	2 Al (10)	2.862	0.383
	2 Al (20)	3.078	0.167
	14, polyhedron (23)		

8(*a*), 000, *etc*; accounting for 1152 atoms. Eight more atoms Mg(23) have to be added, each of them at the center of a Friauf polyhedron *F*5 that can be recognized on the packing map Fig. 10; each *F*5 polyhedron shares edges with twelve *F*3 polyhedra and lies at the center of a sphere as is shown in Figs. 8 and 9. With the addition of 32 more atoms, 32 Al(21), out from the centers of the triangles of eight such *F*5 polyhedra (see Fig. 10), the entire complement of 1192 atoms in the ordered structure is accounted for.

The disordered model

The disordered model is obtained by replacing every other *F*5 polyhedron and the four associated Al(21) atoms with a centered pentagonal prism [Mg(23)+4Al(9)+4Al(8)+2Al(10)] that has two atoms Al(8) at the poles and two atoms Al(20) out from the centers of two prism faces; this complex of 15 atoms will here be called a *CPP* (a few additional adjustments are required; see below). With the origin chosen as in the packing maps (Figs. 12–17), four *CPP*'s are centered at $\frac{113}{444}$, $\frac{131}{444}$, $\frac{311}{444}$, and $\frac{333}{444}$; the *F*5 polyhedra are at $00\frac{1}{2}$, $0\frac{1}{2}0$, $\frac{1}{2}00$, and $\frac{111}{222}$. Only the *CPP* at $\frac{113}{444}$ and the *F*5 polyhedra at $00\frac{1}{2}$ and $\frac{111}{222}$ are shown in these Figures.

The space group symmetry* is effected through a random occurrence of the six orientations of the *CPP*'s shown in Figs. 12–17 and through random interchange of the set of four *F*5 polyhedra [+4 Al(21)] and the set of four *CPP*'s in the individual unit cells.

In a similar fashion as each *F*5 polyhedron is shared between twelve *F*3 polyhedra, each *CPP* is shared between twelve modified Friauf polyhedra, namely 2*F*3*a*, 2*F*3*b*, 4*F*3*c*, and 4*F*3*d*, which are described in the next section.

The T_d complex shown in Fig. 4 has now to be modified. Of any two diametrically opposed *VF* polyhedra in this complex, one remains unchanged while the other contains, instead of two *F*3 polyhedra, two modified Friauf polyhedra; these are either 2*F*3*a*, 2*F*3*b*, or *F*3*c*+*F*3*d*. In the three-dimensional network of the altered T_d complexes each second sphere of the kind shown in Fig. 9 will then have a *CPP* (15-atom complex) at its center instead of the *F*5 polyhedron with the 4 Al(21) (21-atom complex). Since there are four spheres of each kind per unit of structure, the total number of atoms is $1192-4(21-15)=1168$.

Replacement of four *F*5 polyhedra by four *CPP* groups requires that 24 of the originally assumed 96 Mg(11) atoms be replaced by Al(12) atoms which are smaller. In Figs. 12–17 each point of the set reserved for Mg(11) or Al(12) is represented with a dot if occupied but with a small circle if vacant. In Fig. 12, for example, in which the *CPP* is oriented with its pentagonal axis perpendicular to the drawing, there is ample room for one Mg(11) atom on either side (the blank area is partially overlapped by Mg(13) atoms not shown here); in Fig. 13, however, in which the pentagonal axis is horizontal in the plane of the drawing, the presence of Al(8) requires that the two Mg(11) atoms be replaced by Al(12) at slightly different positions. The dotted circular disc around each Al(8) at the extended

* It should be emphasized that a careful inspection of the Weissenberg photographs revealed no reflections that violated the space group symmetry. No diffuse reflections of small disordered domains were found and the measured intensities apparently correspond almost entirely to coherent interference, as is indicated by the good *R* index; concealed twinning is also unlikely.

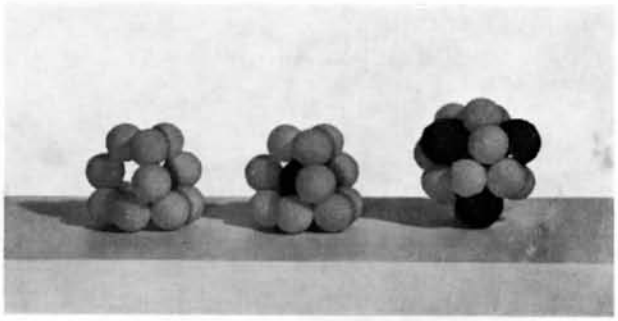

(*a*) (*b*) (*c*)

Fig. 2. (*a*) (*b*) The truncated tetrahedron.
(*c*) The Friauf polyhedron.

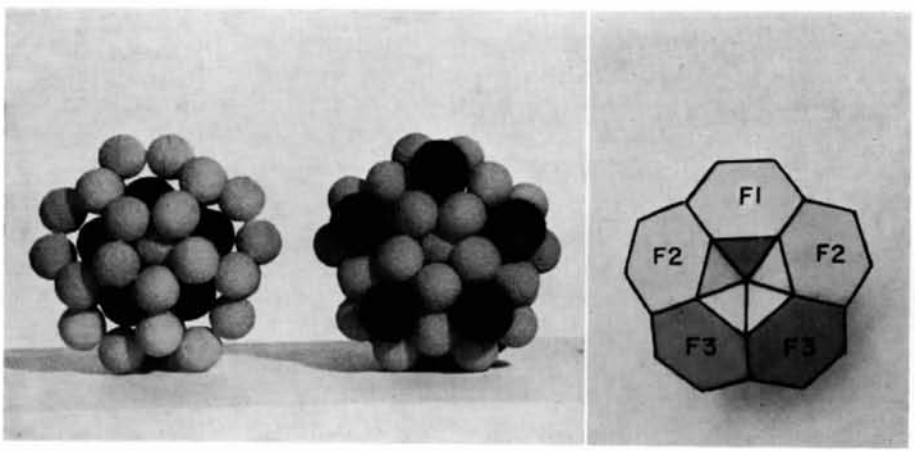

(*a*) (*b*) (*c*)

Fig. 3. (*a*) Five truncated tetrahedra about a fivefold axis of symmetry. (*b*) The *VF* polyhedron. (*c*) A formal representation of the *VF* polyhedron. For the sake of perspicuity, the atoms out from the centers of the hexagons are not indicated.

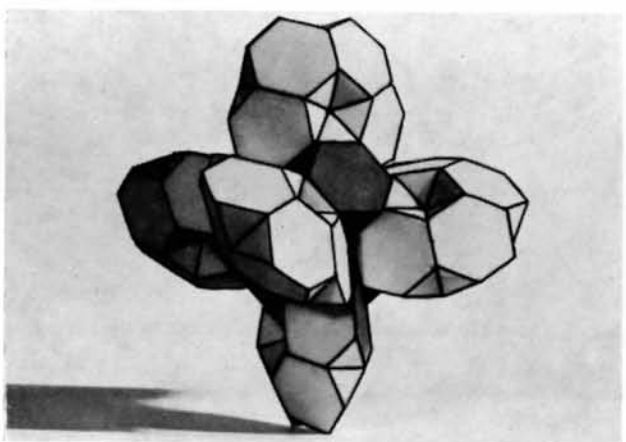

Fig. 4. The 234-atom complex formed by six *VF* polyhedra which are arranged around the vertices of an octahedron of T_d symmetry. In the disordered model six of the twelve outermost Friauf polyhedra are distorted; see text.

[*To face p.* 408

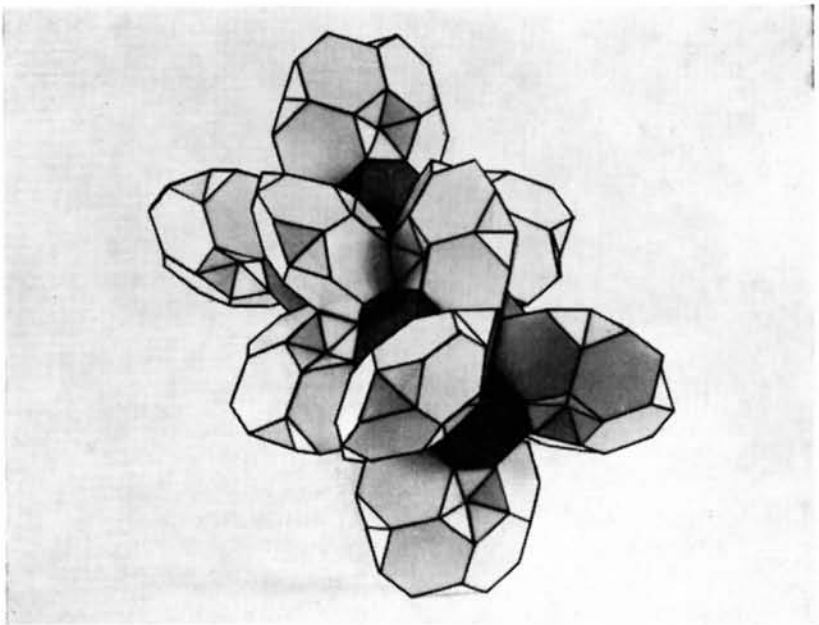

Fig. 5. A second 234-atom complex inserted into the one shown in Fig. 4.

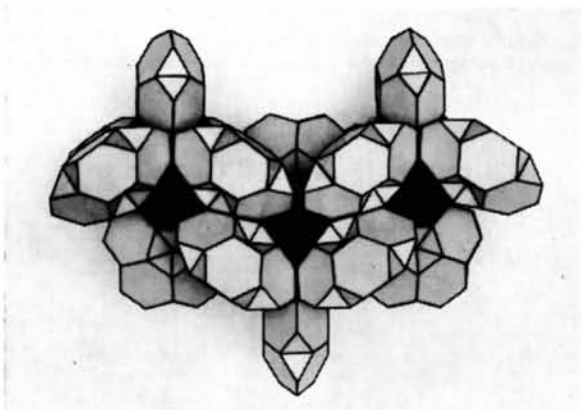

Fig. 6. Three 234-atom complexes forming part of the aggregate shown in Fig. 7.

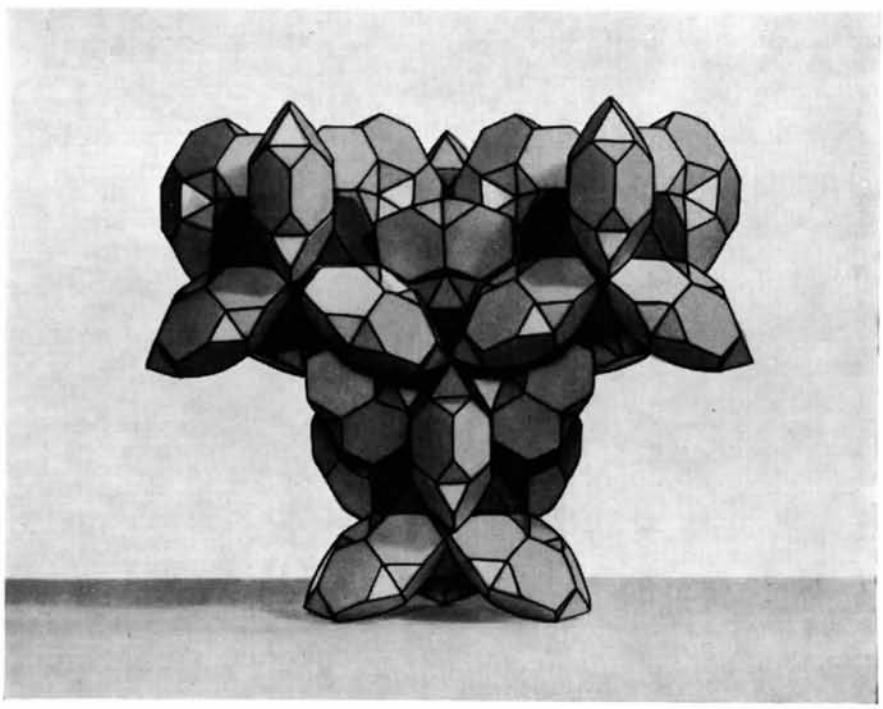

F ig. 7. Four 234-atom complexes arranged about one such complex. The four complexes are at the vertices of a regular tetrahedron.

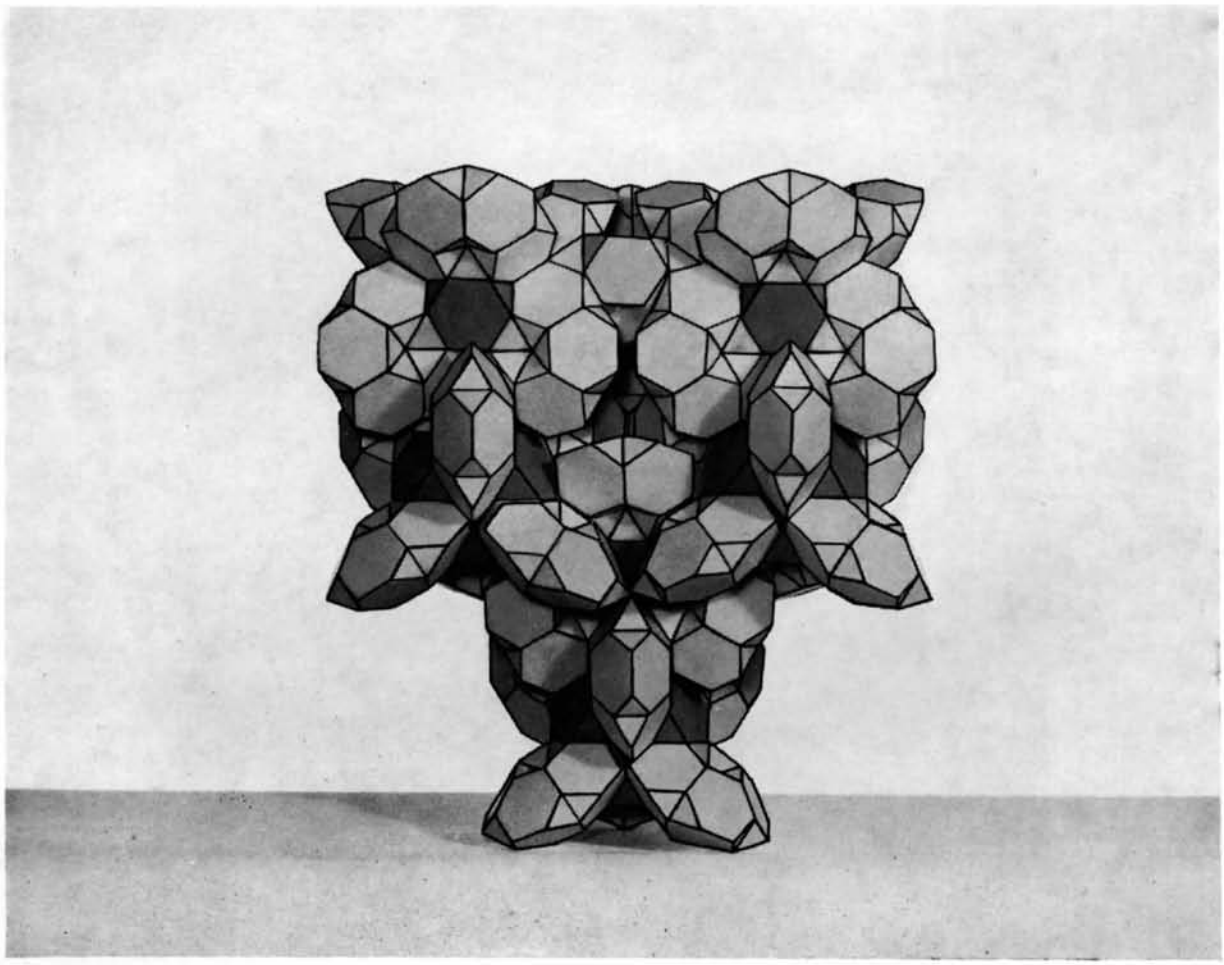

Fig. 8. Continued stacking of the 234-atom complexes leads to the configuration shown above. The sphere shown in Fig. 9 can be recognized here. Its center is located about two-thirds up the vertical center line of this figure.

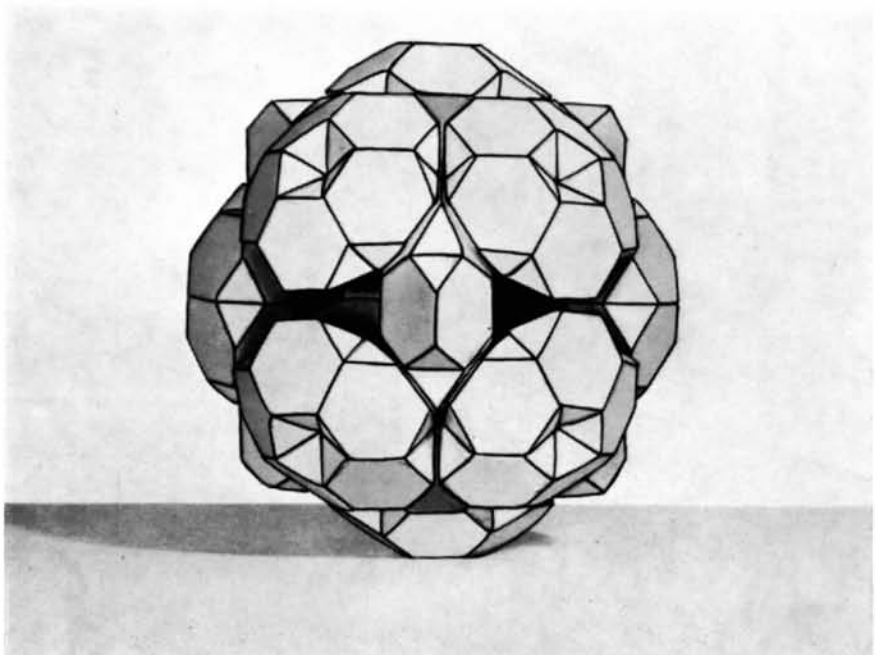

Fig. 9. Twelve *VF* polyhedra (4 × 3) form a sphere around each one of the eight points $00\frac{1}{2}$, *etc*. Six additional *VF* polyhedra are arranged about the vertices of a second kind of T_d octahedron, that can be made out on this Figure. The Friauf polyhedron *F*5, which is shared between these *VF* polyhedra, is at the center of this sphere.

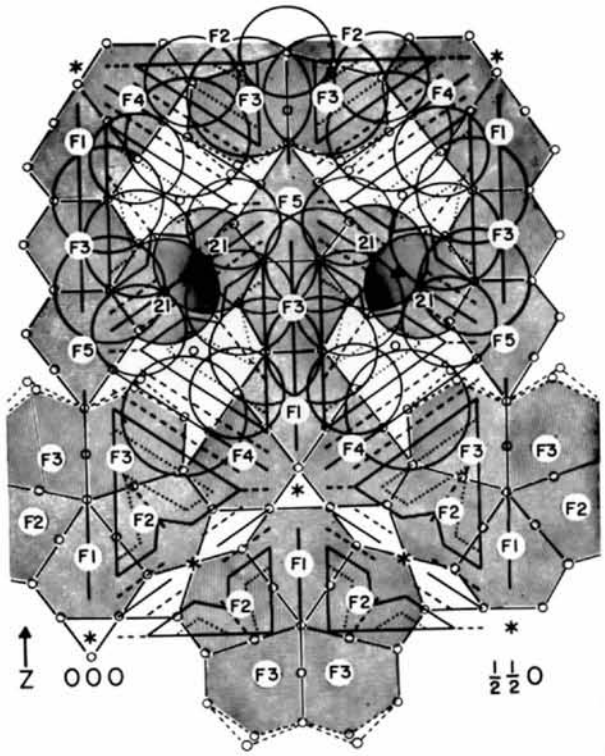

Fig. 10

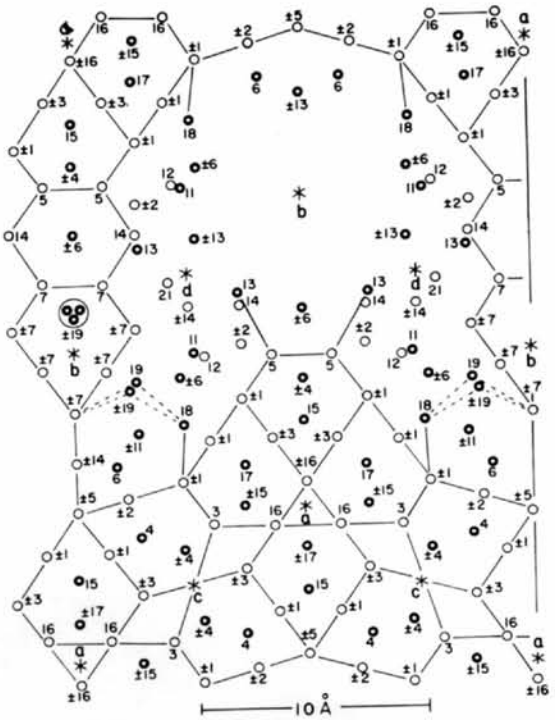

Fig. 11

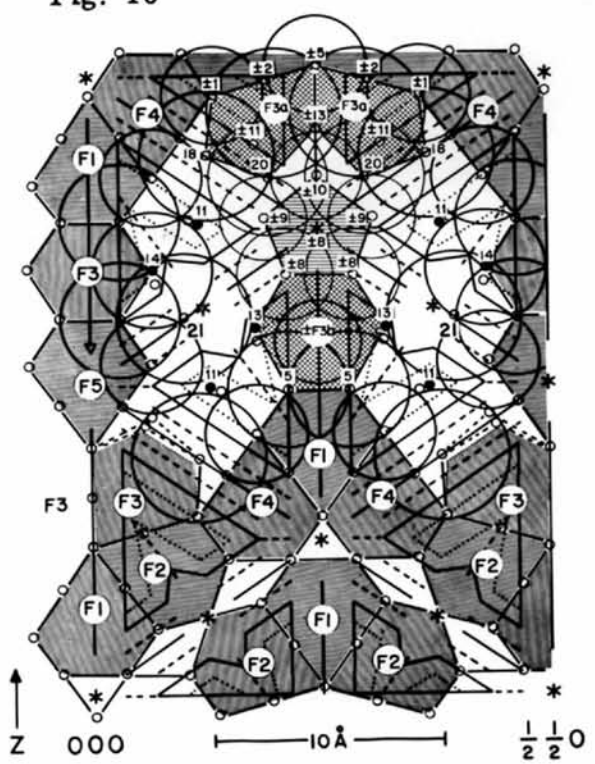

Fig. 12

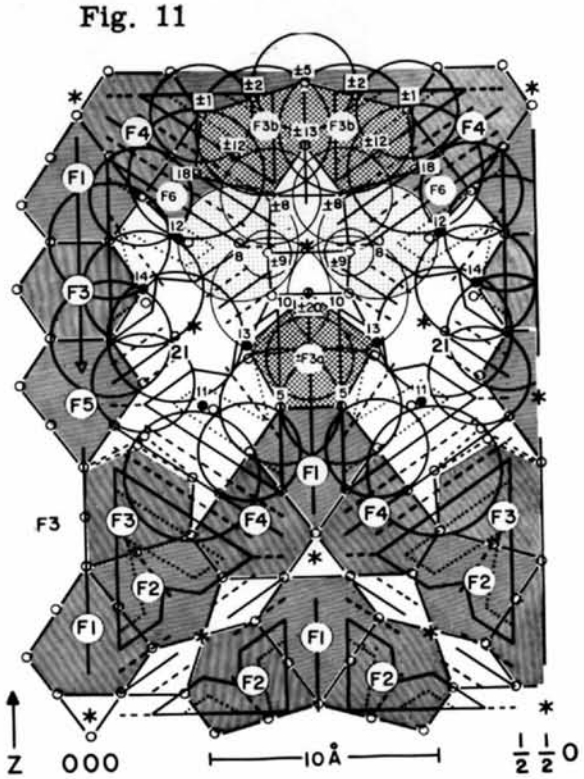

Fig. 13

Fig. 10. Packing map of the idealized ordered model of β Mg_2Al_3.

Fig. 11. Auxiliary map for the identification of the crystallographically different atoms on the packing maps. The number near each circle represents the same atom number as in Table 1. Heavy circles: Mg, light circles: Al. The atoms incorporated in the *CPP* have been left out.

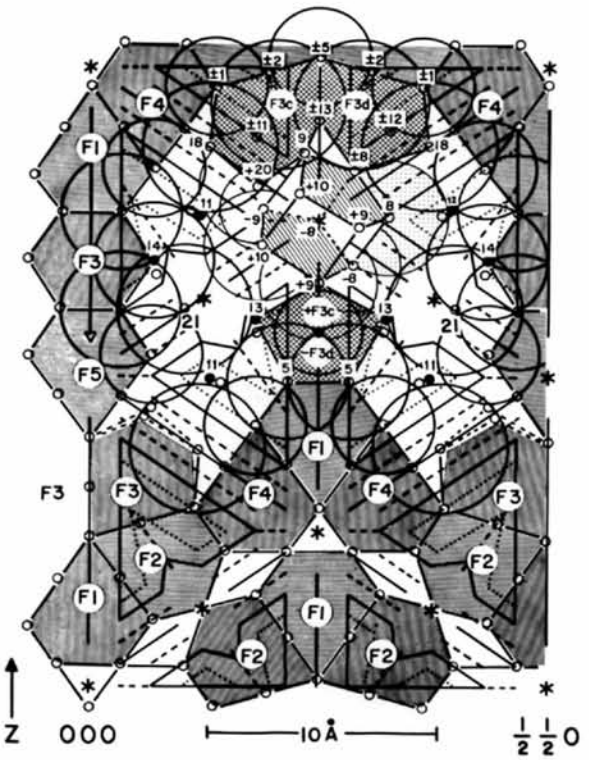

Fig. 14

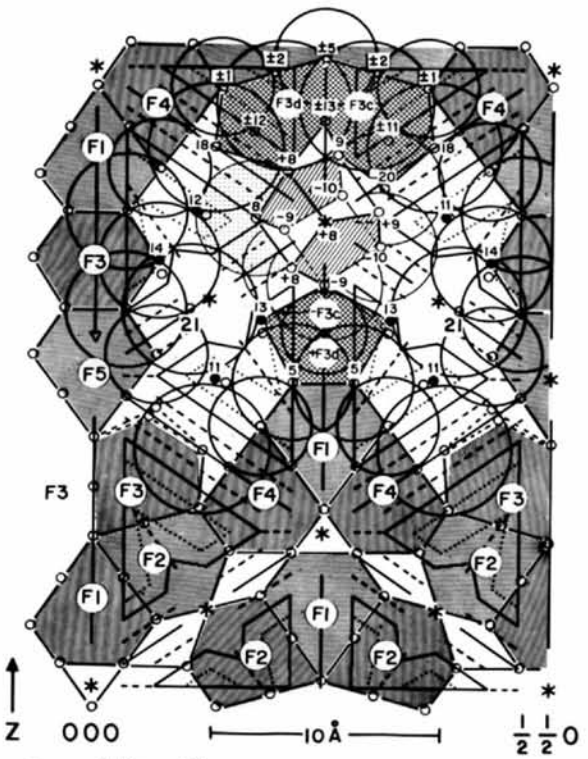

Fig. 15

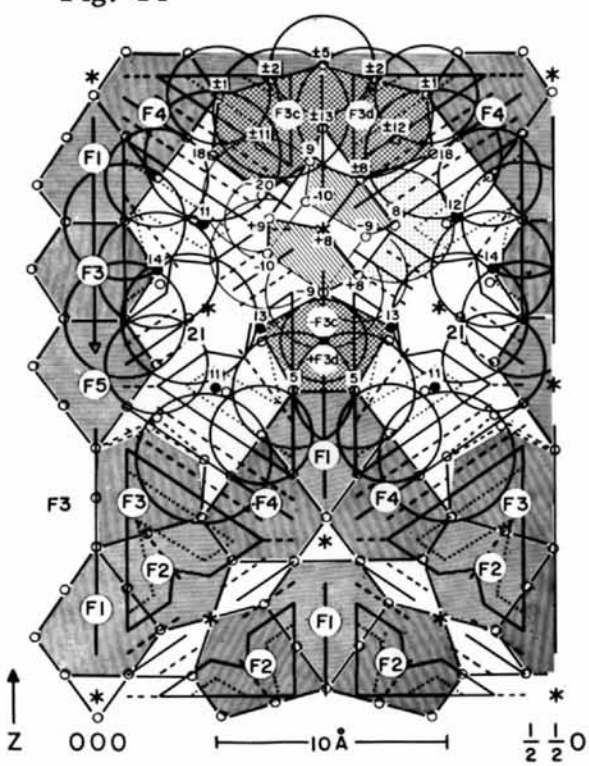

Fig. 16

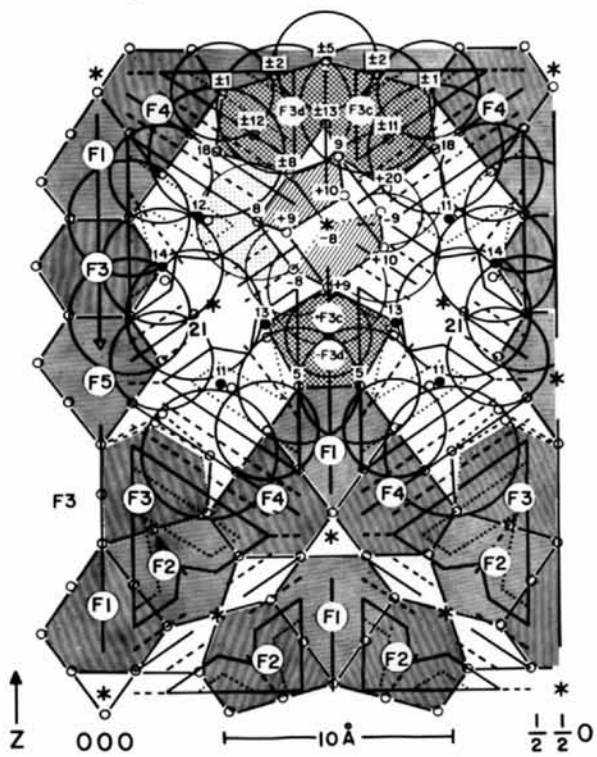

Fig. 17

Figs. 12 to 17. The six packing maps of the disordered model showing the different orientations of the 15-atom complex, the centered pentagonal prism with two atoms, 2 Al(8), at the poles and two atoms, 2 Al(20), out from the centers of two prism faces. The filled circle of each of the two pairs Mg(11)–Al(12) and Mg(13)–Al(14) respectively represents the member of each pair that is present at the instant of time. Alternatively the six packing maps represent a single orientation of the *CPP* projected on the six (110) planes that intersect at the point $\frac{1}{4}\frac{1}{4}\frac{1}{4}$.

pentagonal axis (pole) has a radius corresponding to 2·65 Å, an average Al–Al distance; it is seen that the disc overlaps the small circle [Mg(11)] but not the dot [Al(12)]. In Figs. 14 and 16 Mg(11) is present on the left side and Al(12) on the right side of the *CPP*, while in Figs. 15 and 17 Mg(11) is on the right side and Al(12) on the left side. Each *CPP* is accordingly surrounded by 6 Mg(11) and 6 Al(12) and the four *CPP* groups per unit cube account for 24 Mg(11) and 24 Al(12). The remaining 48 Mg(11) atoms, which lie near $z=\frac{1}{2}$ in Figs. 12–17, are unaffected by the disorder.

Mg(13) and Al(14) are represented in the six figures in accordance with the same principle. Al(14) is always associated with the Friauf polyhedra *F*3 while Mg(13) belongs to the modified Friauf polyhedra *F*3*a*, *b*, *c*, *d*. The possible additional displacement of Mg(13) suggested in the refinement section is easily recognized in Fig. 13.

Finally, only one half of the set of 32 points assigned Mg(19) in the ordered model remain as vertices of *F*3 polyhedra. Of the other sixteen points, eight are unoccupied and eight are located out from centers of prism faces of the *CPP* groups (two points per *CPP*), and can only be occupied by small atoms [Al(20)], slightly displaced from the diagonals (*xxx*, *etc.*). The positions of these Al(20) atoms for the six different orientations of the *CPP* can be seen in Figs. 12–17; it is also seen that the sixteen Mg(19) atoms are slightly displaced from the diagonals (*xxx*, *etc.*), where they were originally assumed.

Some interesting features of the disorder as revealed through detailed analysis of the coordination polyhedra will be discussed in the final section.

Discussion of the coordination polyhedra

As a result of the disorder, the 23 crystallographically different atoms produce 41 different polyhedra. Accordingly, some atoms have more than one set of ligands, the maximum number of sets per atom being five for Mg(6). The ligands and the center-to-vertex distances of these polyhedra are listed in Table 3.

The polyhedra of ligancy 10, 11, *and* 12

All except 24 of the 720 aluminum atoms in the unit of structure have ligancy 12. Of these 24, sixteen have ligancy 11 and eight have ligancy 10. Of the polyhedra providing ligancy twelve, 672 are icosahedra and 24 are irregular.

In this structure, as in most other intermetallic compounds, the icosahedra are somewhat distorted. The 672 icosahedral shells observed here are of sixteen different kinds; the first thirteen kinds (Table 4) have between 9 and 11 crystallographically different atoms and between 12 and 19 parameters each, while the remaining three incorporate between 2 and 4 different atoms and between 4 and 8 parameters each. Since in a cubic crystal no more than four threefold axes can intersect at one point, at least six of the ten threefold axes of the icosahedron must be non-crystallographic. In fact, only the last three isosahedra in Table 4 have one crystallographic threefold axis each; the others have none.

Table 4. *Some metrical data on the icosahedra observed in β* Mg_2Al_3

ID = identification number (see Table 3), *N* = number of icosahedra per unit cell, *E* = average length of the thirty edges, *D* = average value of the twelve center-to-vertex distances, Mg, Al = number of respective atom at the vertices, *v* = calculated valence of central atom.

ID	*N*	*E*	*D*	*D*/*E*	Mg	Al	*v*
1*a*	144	3·165	2·990	0·945	7	5	2·94
1*b*	48	3·132	2·961	0·945	6	6	3·15
2*a*	72	3·144	2·974	0·946	5	7	2·96
2*b*	24	3·112	2·957	0·950	6	6	3·03
3	96	3·131	2·965	0·947	6	6	2·91
5*a*	48	3·166	2·994	0·946	5	7	2·99
5*b*	24	3·115	2·945	0·946	6	6	3·49
5*c*	24	3·075	2·913	0·947	5	7	3·58
7	48	3·128	2·977	0·952	7	5	3·07
8*a*	8	3·238	3·060	0·945	6	6	2·67
12	24	3·101	2·951	0·952	5	7	2·91
14*a*	24	3·129	2·957	0·945	5	7	3·44
14*b*	24	3·119	2·949	0·946	6	6	3·43
16	32	3·113	2·951	0·948	6	6	2·96
21	16	3·132	2·969	0·948	6	6	2·88
22	16	3·122	2·959	0·948	6	6	2·92
	672						

The radius of the magnesium atoms as calculated on the basis of Pauling's (1947) paper is about 14% greater than that of the aluminum atoms, if allowance is made for the ligancies observed here. Since the radius of the central sphere of a regular icosahedron is only about 10% smaller than the radius of the twelve contiguous spheres at the vertices, it is not surprising that in each icosahedral shell observed here about half the vertices are occupied by magnesium atoms and the other half by aluminum atoms (columns 6 and 7, Table 4). This distribution of atoms, which in part accounts for the deformation of the icosahedral shells, provides a very efficient packing around each central aluminum atom. The variation in the values of *E* (average edge) and *D* (average center-to-vertex distance) given in Table 4 probably arises to some extent from the fact that each icosahedral shell has to comply not only with the coordination requirements of the central atom but also with the coordination requirements of the atoms at the vertices. Thus the successive decrease in the values of *E* and *D* for the icosahedra 5*a*, 5*b*, and 5*c*, Table 4, appears to be due to a successive increase of the number of icosahedra that in turn interpenetrate each of these coordination shells. The polyhedron 5*a* has five icosahedral aluminum atoms at the vertices, while 5*b* has six and 5*c* has seven. Of the remaining atoms at the vertices of each of the three isocahedra, five are surrounded by Friauf polyhedra or modified Friauf polyhedra and the rest by irregular polyhedra of ligancy 15, as in the icosahedron 5*a*, or ligancy 14, as in the icosahedron 5*b*. Each of the polyhedra 3, 16,

and 22 (Table 4) are interpenetrated by six icosahedra and six Friauf polyhedra. The icosahedron 8*a* (Table 4) has only one interpenetrating icosahedron; it also has the largest volume.

The ratios D/E given in Table 4 deviate somewhat from the value 0·951 calculated for the regular icosahedron. This may be expected on account of the deformation. The only two coordination shells of ligancy twelve that are not icosahedral (Table 5) correspond to a radius ratio of nearly unity, $(D-0{\cdot}5E)/0{\cdot}5E \simeq 0{\cdot}98$.

Table 5. *Irregular coordination shells of ligancy* 12 *and less*

L = ligancy; all other column headings have a similar meaning to those in Table 4.

ID	N	L	E	D	D/E	Mg	Al	v
8*b*	16	11	3·228	3·124	0·968	6	5	1·96
9	16	12	3·097	3·075	0·993	7	5	3·43
10	8	12	3·078	3·027	0·983	5	7	3·22
20	8	10	3·258	2·919	0·896	6	4	3·73
	48							

The atomic configurations around the remaining 48 aluminum atoms are as follows (Table 5):

8*b*: Ligancy 11. Similar to the icosahedron 8*a*, but considerably distorted and with one vertex removed. The distortion causes the coordination shell to remain closed after removal of that vertex (atom).

9: Ligancy 12. Icosahedron, in which two vertices, Al(9) and Al(20), have been shifted.

10: Ligancy 12. Distorted tetragonal prism in which two atoms penetrate prism faces and two atoms penetrate edges that are parallel to the prism axis.

20: Ligancy 10. A cube that has been distorted so as to permit two more atoms, 2 Al(10), to be in contact with the central atom through two of the cube faces. Out from the centers of two of the less distorted cube faces are two more atoms, 2 Mg(6), at a distance of 3·887 Å from Al(20). These two atoms correspond to the long-distance neighbors in the *A*2 structures and are not included here as ligands.

The Friauf polyhedra

The unit of structure contains 252 Friauf polyhedra [Fig. 2(*c*)] of seven different kinds (*F*1–*F*7). For each Friauf polyhedron the first twelve ligands listed in Table 3 constitute the truncated tetrahedron [Fig. 2(*a*), (*b*)] and the last four ligands the surrounding negative tetrahedron, except for *F*6 and *F*7, for which this kind of listing is inconvenient. *F*6 is shown only partially in Fig. 13 but it can be traced out easily. *F*7 can be made out with the aid of Figs. 11 and 14, if the centers of the atoms around Mg(13) are laid out on a tracing paper. One can then recognize a hexagonal antiprism with one atom, Mg(11), out from the center of one hexagon, and three atoms, −Al(8), +Al(9), and +Al(10), out from the center of the other hexagon. This is an alternative description of the Friauf polyhedron. The atom −Al(8) out from the center of the pentagon of the *CPP* (see section on disordered model) is not marked out in Fig. 14.

Except in the case of *F*5, each truncated tetrahedron shares one or more hexagons with adjacent truncated tetrahedra such that the number of different hexagons totals fourteen. The planarity and regularity of the fourteen hexagons are indicated in Table 6. The most deformed hexagons are Hex. 5, 6, 10, and 11 (see below). The four hexagons that form each truncated tetrahedron are identified in columns 7 to 10 in Table 7; the dihedral angle between pairs of adjoining hexagons are given in columns 11 and 12.

Table 6. *Planarity and regularity of the hexagons of the truncated tetrahedra*

Column 2 gives the maximum deviation from each least-squares plane; columns 3 and 4 give the smallest and largest interior angle, and columns 5 and 6 the shortest and longest side of each hexagon.

	Max. dev.	Interior angles		Sides (Å)	
Hex. No.	Å	min.	max.	min.	max.
1	0·008	118·3	122·0	2·601	2·853
2	0·021	118·7	121·3	2·696	2·778
3	0·004	118·4	121·2	2·601	2·755
4	0·007	117·8	120·9	2·696	2·761
5	0*	114·0	123·6	2·598	2·715
6	0·126	116·4	123·6	2·705	3·038
7	0*	120·0*	120·0*	2·719	2·725
8	0·021	118·7	121·3	2·696	2·778
9	0*	120·0*	120·0*	2·598	2·807
10	0·081	115·5	130·1	2·648	2·948
11	0·313	114·8	122·5	2·509	3·164
12	0·000	109·0	130·6	2·509	3·019
13	0·202	110·5	124·5	2·652	2·754
14	0·132	111·4	128·3	2·573	2·060

* Required by symmetry.

It can be seen (Tables 6 and 7) that the shortest and longest of the 18 edges of the truncated tetrahedron of *F*1 are 2·601 Å and 2·853 Å, and that the dihedral angles are very nearly tetrahedral. The regularity of the truncated tetrahedra of *F*2, *F*4, and *F*5 is comparable to that of *F*1, while *F*3, *F*6, and *F*7 are quite distorted.

Table 8 includes the atoms at the vertices of the negative tetrahedron around each truncated tetrahedron; here, E is the average of the $18+24=42$ edges and D the average of the sixteen center-to-vertex distances. Columns 5 and 6 give the minimum and maximum of the six bond angles between the atoms at the vertices of the negative tetrahedron and the central atom. It is seen, again, that, with the exception of *F*3, *F*6, and *F*7, these bond angles are nearly tetrahedral.

The atoms Mg(19), which form the negative tetrahedron around *F*5, are displaced from the diagonal as has been pointed out earlier. The tetrahedral angles of *F*5 are therefore omitted in Table 8. The calculations for Hex. 6 (Table 6) were made with Mg(19) placed at its average position; that is, on the body diagonal.

The truncated tetrahedron of *F*3 has the interesting feature that two of its vertices, Mg(18) and Mg(19), constitute simultaneously the sites of the atoms out

Table 7. *Metrical data and dihedral angles of the truncated tetrahedra*

ID = identification number, N = number of polyhedra per unit cell, E = average length of the eighteen edges, D = average value of the twelve center-to-vertex distances, a, b, c, d = the four hexagons (see Table 6) forming the truncated tetrahedron.

ID	Central atom	N	E	D	D/E	Kind of hexagon a	b	c	d	Dihedral angles $a{\cdot}b$	$c{\cdot}d$
$F1$	Mg(15)	48	2·739	3·203	1·169	1	1	2	2	70·8	71·2
$F2$	Mg(4)	96	2·727	3·191	1·170	1	3	4	4	70·9	71·3
$F3$	Mg(6)	48	2·776	3·235	1·165	3	5	6	6	73·7	66·0
$F4$	Mg(17)	32	2·727	3·201	1·174	2	7	8	8	70·9	70·2
$F5$	Mg(23)	4	2·737	3·181	1·162	9	9	9	9	70°32′*	70°32′*
$F6$	Mg(18)	8	2·764	3·232	1·169	7	10	10	10	72·1	69·0
$F7$	Mg(13)	16	2·800	3·268	1·167	11	12	13	14	66·4	68·6
		252									

* Tetrahedral by symmetry requirements.

Table 8. *Metrical data and bond angles of the Friauf polyhedra*

E = average length of the 42 edges, D = average value of the sixteen center-to-vertex distances, v = calculated valence of central atom. In columns 5 and 6 are given the minimum and maximum of the six bond angles between the atoms out from the centers of the four hexagons and the central atom

ID	E	D	D/E	Tetrahedral angles min.	max.	v
$F1$	2·989	3·227	1·080	107·1	110·3	1·70
$F2$	2·984	3·222	1·079	108·0	111·1	1·74
$F3$	3·001	3·238	1·079	106·9	112·0	1·97
$F4$	2·973	3·214	1·081	108·3	110·7	1·85
$F5$	2·913	3·154	1·083	—	—	2·41
$F6$	3·045	3·285	1·079	106·0	112·8	1·93
$F7$	3·031	3·263	1·077	107·0	117·0	2·09

from the centers of the hexagons of $F4$ and $F5$, respectively (Figs. 10 to 17). The two vertices are also at quite a distance, about 3·5 Å, from the center, Mg(6). A similar feature is observed for one of the two Friauf polyhedra in the γ $Mg_{17}Al_{12}$ structure ($A12$ structure; Laves, Löhberg & Rahlfs, 1934). The coordination shells around Mg(18) and Mg(19) are also the same as the one observed in γ $Mg_{17}Al_{12}$ (ligancy 14; see below). This analogy was helpful for the synthesis of the first model. It was believed, however, that each of the five Friauf polyhedra $F1$, $2\times F2$, and $2\times F3$ arranged around the fivefold axis of symmetry would assume nearly the same dihedral angle of $360°/5=72°$ and, furthermore, that some irregularities would distribute themselves evenly among all five polyhedra in the course of the structure refinement. It is now seen, however, that the dihedral angles of $F1$ and $F2$ ($a\,.\,b$ in column 11, Table 7), are nearly tetrahedral and that about 85% of the discrepancy ($360°-5\times 70·5°=7·5°$) is accumulated in the two contiguous polyhedra $F3$. Hence, there is tendency toward strict tetragonality among $F1$, $F2$, $F4$, and $F5$, which results in a misfit of the polyhedra $F3$.

The modified Friauf polyhedra

The four modified Friauf polyhedra are briefly described as follows; see also Table 9.

Table 9. *Metrical data on miscellaneous kinds of polyhedra*

The column headings have a similar meaning to those in Table 7.

ID	N	L	E	D	D/E	v
11a	8	13	3·027	3·127	1·033	2·82
11b	16	14	3·060	3·274	1·070	3·12
13b	8	14	3·116	3·179	1·020	3·72
18a	16	14	3·126	3·173	1·015	2·74
18b	8	14	3·132	3·179	1·015	2·33
19	16	14	3·112	3·172	1·019	3·48
23	4	14	2·875	3·004	1·045	3·21
F3a	8	14	3·054	3·223	1·055	2·01
F3c	16	14	3·059	3·191	1·043	2·96
F3b	8	15	3·060	3·273	1·070	1·65
11c	48	15	3·013	3·171	1·052	2·27
13a	8	15	3·049	3·255	1·068	1·65
13c	16	15	3·050	3·248	1·065	2·06
F3d	16	16	3·060	3·274	1·070	1·72
	196					

F3a: Ligancy 14; see Fig. 12. Same as $F3$ except for the following alterations: (1) The vertex Mg(19) has been replaced by Al(20) which is still farther displaced from the body diagonal of the cube such as to reduce the center-to-vertex distance from about 3·5 Å to 3·021 Å; (2) the two atoms, 2 Al(14), have been replaced by 2 Mg(13); (3) the two vertices, 2 Al(7), have been replaced by 2 Al(10), which are at quite a distance, 3·8 Å, from the center and are shielded by Al(20) and 2 Mg(13). These two atoms are not regarded as ligands of the central atom Mg(6).

F3b: Ligancy 15; see Fig. 13. Same as *F3a* except that Al(20) has been replaced by 2 Al(8) and as a consequence thereof, 2 Mg(11) have been substituted by 2 Al(12) to avoid interference. Compare Fig. 13 with Fig. 12.

F3c: Ligancy 14; see left side of Figs. 14 and 16 and right side of Figs. 15 and 17. Same as *F3a* except that Al(20) now occupies a different corner of the small equilateral triangle around the body diagonal of the cube and therefore is at a distance of 3·89 Å from the central atom Mg(6). The atom Al(9) has taken over its function as a ligand.

Al(20) remains always above the center of the prism face of the pentagonal prism and flips from one corner

of the equilateral triangle to the other as the pentagonal prism changes orientation.

*F*3*d*: Ligancy 16; see right side of Figs. 14 and 16 and left side of Figs. 15 and 17. Same as *F*3*b* except that Al(9) has been added as the sixteenth ligand.

The remaining ten coordination shells

The ten coordination shells not yet discussed are listed in Table 9 in sequence of increasing ligancy together with the modified Friauf polyhedra just described. A brief discussion is given below.

11*a*: Ligancy 13; see at $z\sim\frac{3}{4}$ in figures referred to below. Pentagonal antiprism in which the two pentagons are of different size. The small pentagon consists of Al(14), ±Al(2), and ±Al(1) and the large pentagon of Mg(18), ±Mg(13) and ±Mg(6) (Fig. 11). Out from the center of the small pentagon is Al(5) and outside the large pentagon are two atoms, ±Al(9); see Fig. 12.

11*b*: Ligancy 14; see at $z\sim\frac{3}{4}$ in figures referred to below. Same as 11*a*, except that there are three atoms, +Al(9), −Al(10), and −Al(20), out from the center of the large pentagon; see right side of Figs. 15 and 17 and left side of Figs. 14 and 16. In Figs. 14 and 17 we have −Al(9), +Al(10), and +Al(20) but the coordination polyhedron remains the same.

11*c*: Ligancy 15; see at $z\sim\frac{1}{2}$ in the figures referred to below. Same as 11*b*, but the two magnesium atoms ±Mg(13) of the larger pentagon have been replaced by ±Al(14) that are at a larger distance from the (110) plane such that now four atoms, ±Al(7), Mg(19), and Al(21) penetrate this pentagon and make contact with the central atom. In the small pentagon, the aluminum atom Al(14) has been replaced by Mg(13). This polyhedron is present in all six cases, Figs. 12 to 17. and is most easily made out with the aid of Fig. 11,

13*a*: Ligancy 15; see Fig. 12. Hexagonal antiprism with one atom, Mg(11), out from the center of one hexagon and two atoms, ±Al(8), outside the other hexagon. This polyhedron is a modification of Friauf polyhedron *F*7.

13*b*: Ligancy 14; see Fig. 13. Hexagonal antiprism with two atoms, Mg(11) and Al(10), at the poles.

13*c*: Ligancy 15. The configuration is the same as that of 13*a* but the atom +Al(8) has been substituted by +Al(9) and one vertex of the hexagonal antiprism is occupied by Mg(11) instead of Al(12); see right side of Figs. 14 and 16 and left side of Figs. 15 and 17. In Figs. 15 and 16 we have −Al(9) instead of +Al(9) but the polyhedra are the same.

18*a*: Ligancy 14. Hexagonal antiprism with two atoms, Mg(19) and Mg(17), at the poles. These polyhedra are at $z\sim\frac{1}{2}$ in Figs. 12 to 17.

18*b*: Ligancy 14. Same as 18*a* except that Mg(19) has been replaced by Al(20); see at $z\sim\frac{7}{8}$ in Fig. 12 and left side of Figs. 14 and 16 or right side of Figs. 15 and 17. Opposite to each one of the polyhedra 18*b* in the last four figures is the Friauf polyhedron *F*6.

19: Ligancy 14; see at $z<\frac{1}{2}$ in Figs. 12 to 17. Hexagonal antiprism with two atoms, Mg(18) and Mg(23) at the poles.

23: Ligancy 14. This polyhedron referred to as the *CPP* has been discussed extensively in preceding sections.

The bond distances and packing of atoms

The interatomic distances are listed in Table 3 together with the bond numbers n calculated with the use of the equation $D_n = D_1 - 0{\cdot}600 \log_{10} n$ and the single-bond radii given by Pauling (1947). The calculated valences are given in the Tables 4, 5, 8, and 9.

The shortest distances observed in this structure are Mg(6)–Al(9) = 2·57 Å and Mg(13)–Al(10) = 2·51 Å. It has already been pointed out (see section on refinement) that Mg(13) is probably displaced part of the time, and accordingly some of the distances involving this atom cannot be evaluated properly. A second uncertainty in the bond numbers arises from the difficulty to determine by X-ray techniques the exact distribution of the magnesium and aluminum atoms over the occupied positions; the possibility of partially random occupancy by magnesium and aluminum has to be kept in mind.

The values of E, D, and D/E in Tables 4, 5, 8, and 9 may serve as a guide for estimating the relative packing efficiencies. The icosahedra correspond to a radius ratio of 0·90, the Friauf polyhedra to a radius ratio of 1·16, while for the various miscellaneous polyhedra listed in Table 9 this ratio varies between 1·03 and 1·14.

On the nature of the disorder

Although it appears from Figs. 2 to 9 that the Friauf polyhedra are dominant in this structure, they are by far outnumbered by the icosahedra. In recent years it has become ever more apparent that, of the coordination shells of ligancy twelve, the icosahedron is the one that corresponds to maximum stability if atoms of slightly different sizes are involved. This coordination shell is present in almost every complex cubic intermetallic compound, the complexity probably arising from the difficulty of fitting the polyhedra with fivefold axes of symmetry into a crystal with cubic symmetry (Pauling, 1964). The complexity is here enhanced because the closest possible packing apparently requires that each icosahedral shell is made up of atoms of two different sizes (see under polyhedra above), the larger atoms in turn requiring a ligancy greater than twelve.

The disorder observed here seems to be the result of the tendency towards the formation of the maximum number of icosahedral coordination shells that is compatible with the coordination requirements of the magnesium atoms. Eighty-eight of the coordination shells that in the idealized ordered model were more-or-less irregular have been transformed into the icosahedra

12, 14*a*, 14*b*, and 21 (Table 4), forty-eight of the original ninety-six icosahedra around Al(7) have been lost (50% occupancy), and eight icosahedra (8*a*) have been added. There is accordingly a gain of forty-eight icosahedra per unit of structure, and the apparent requirement of having about half the vertices occupied by magnesium atoms and the other half by aluminum atoms is fulfilled through the splitting of the atoms Mg(11) and Al(14) into the pairs Mg(11)–Al(12) and Mg(13)–Al(14) respectively. While the idealized ordered model* contains 280 Friauf polyhedra, 624 icosahedra, and 288 more-or-less irregular polyhedra, the disordered atomic arrangement corresponds to 252 Friauf polyhedra, 672 icosahedra, and 244 more-or-less irregular polyhedra of ligancy 10 to 16, of which 48 are modified Friauf polyhedra.

No definite statement can be made whether the disorder is static or dynamic.

Another interesting feature of this structure is the pronounced tendency towards the formation of five-fold axes, not only those of the icosahedra, but also those of the *VF* polyhedra. This striving towards pentagonality is also reflected in the Fourier section shown in Fig. 1.

I thank Professor Linus Pauling for his great interest in this work and Dr R. Marsh for valuable suggestions in preparing the manuscript. I am grateful to Dr R. Marsh, Dr N. Webb, Mr D. J. Duchamp and Mr A. Kendig for providing the IBM 7094 programs. Mr K. Christiansson and Mrs B. Christiansson carried out most of the experimental work and data collection. I am especially grateful for their successful efforts to prepare the single crystals. Mr K. Christiansson prepared the drawings for Figs. 11 to 17. I also thank Professor Gunnar Hägg (University of Uppsala) for supplying me with detailed drawings of the Guinier–Hägg camera.

* The structure of $NaCd_2$ contains 624 icosahedra instead of 528 as was erroneously stated in the paper of Samson (1962); the atoms $96g_5$ in Table 1 of that paper have icosahedral coordination.

References

HUGHES, E. W. (1941). *J. Amer. Chem. Soc.* **63**, 1737.

International Tables for X-ray Crystallography (1952). Vol. I. Birmingham: Kynoch Press.

International Tables for X-ray Crystallography (1962). Vol. III. Birmingham: Kynoch Press.

LAVES, F., LÖHBERG, K. & RAHLFS, P. (1934). *Nachr. Ges. Wiss. Göttingen, Fachgr. IV*, **1**, 67.

LAVES, F. & MÖLLER, K. (1938). *Z. Metallk.* **30**, 232.

PAULING, L. (1947). *J. Amer. Chem. Soc.* **69**, 542.

PAULING, L. (1956). *Theory of Alloy Phases.* p. 220–242. Cleveland, Ohio: Amer. Soc. for Met.

PAULING, L. (1964). *Proc. Nat. Acad. Sci. Wash.* **51**, 977.

PERLITZ, H. (1944). *Nature, Lond.* **154**, 607.

PERLITZ, H. (1946). *Chalmers Tekniska Högskolas Handlingar*, **50**, 1.

RIEDERER, K. (1936). *Z. Metallk.* **28**, 312.

SAMSON, S. (1958). *Acta Cryst.* **11**, 851.

SAMSON, S. (1961). *Acta Cryst.* **14**, 1229.

SAMSON, S. (1962). *Nature, Lond.* **195**, 259.

SAMSON, S. (1964). *Acta Cryst.* **17**, 491.

WEBB, N. C. (1964). *Acta Cryst.* **17**, 69.

Acta Cryst. (1965). **19**, 413

Neutron Diffraction Study of Chemical Order-Disorder in $PtMn_3$*

BY S. S. SIDHU, K. D. ANDERSON AND D. D. ZAUBERIS†
Argonne National Laboratory, Argonne, Illinois, U.S.A.

(*Received* 10 *December* 1964)

A neutron study of the chemical order-disorder in $PtMn_3$ was made by utilizing the nuclear properties of Mn and Pt nuclei. The $b_{Mn} = -0{\cdot}36 \times 10^{-12}$ cm and the $b_{Pt} = 0{\cdot}95 \times 10^{-12}$ cm. In a disordered crystal structure of the stoichiometric $PtMn_3$ alloy, the manganese atoms scatter thermal neutrons 180° out of phase with those of platinum. As a result the structure becomes a nuclear null-matrix, and no diffraction peaks appear in its neutron pattern; however, when even a partial ordering takes place in the structure, diffraction peaks do appear in the pattern, and since their intensities depend upon the degree of ordering, they permit a precise determination of the disorder parameter. Numerical values of the disorder parameter of an ordered and a disordered sample of $PtMn_3$ were determined. The technique of using a nuclear null-matrix to study chemical order-disorder phenomena is described.

Introduction

The crystal structure of the $PtMn_3$ alloy is cubic with 4 atoms per unit cell and $a_0 = 3{\cdot}84$ Å. It is similar to that of $AuCu_3$ which has been extensively used to study order-disorder phenomena for this type of structure. The main feature of the X-ray diffraction pattern of the disordered state is that only the all-odd and all-even Miller-index reflections appear, whereas in the ordered state, in addition to the above reflections, mixed Miller indices or the so-called 'super-structure' reflections appear. This follows from the fact that the structure factor for the disordered state is

* Work performed under the auspices of U.S. Atomic Energy Comission.

† The paper was presented at the Annual Pittsburgh Diffraction Conference, November 4–6, 1964, Mellon Institute, Pittsburgh, Pennsylvania.